First Middle East Conference on Smart Monitoring,
Assessment and Rehabilitation of Civil Structures
8 – 10 February 2011, Dubai, UAE

SMAR 2011

Flexural Behaviour of Hybrid FRP-UHPC Beam: Effect of Different Bond Mechanisms

Donna Chen[1] and Raafat El-Hacha[2]

[1] MSc student, Department of Civil Engineering, University of Calgary, Calgary, Alberta, Canada
[2] Associate Professor, Department of Civil Engineering, University of Calgary, Calgary, Alberta, Canada

ABSTRACT: This paper will describe the experimental investigation of two types of hybrid FRP-UHPC structural members from Phase I and II of development. The beams are 2.9m long and are tested under four-point loading in flexure. The cross-section of the structural members are composed of a thin layer of Ultra-High Performance Concrete (UHPC) cast overtop a pultruded GFRP hollow box section, with a single sheet of either Steel FRP (SFRP) or Carbon FRP (CFRP) bonded on the bottom flange for flexural strengthening. The difference between the Phase I and II specimens is the type of bonding used along the interface between the UHPC layer and the top flange of the GFRP hollow box section. In the Phase I specimens, GFRP shear studs without UHPC embedment on the interior of the GFRP hollow box section as well as a thin layer of moisture insensitive epoxy adhesive applied prior to UHPC casting are used. With the Phase II specimens, GFRP shear studs, embedded through the top flange of the GFRP and into a thin layer of UHPC cast within the interior of the hollow box section, as well as silica sand bonded to the top surface using epoxy adhesive prior to casting of the UHPC are used. Analysis will focus on the performance of the bonding system used as well as comparisons between Phase I and II specimens, and cost effectiveness analysis of the two systems (SFRP and CFRP) in terms of strength improvement and material cost.

1   INTRODUCTION

Investigation into the use of Fibre Reinforced Polymers (FRPs) in Civil Engineering applications has been conducted by various researchers internationally during the past two decades, due to their advantageous material properties, which include low self-weight, high strength and most importantly, resistance to corrosion. Due to the relative newness of this material for structural purposes, as compared to concrete, steel and masonry, the initial costs for production is a deterrent for many designers. In order to minimize the financial impact of initial material procurement and production, hybrid structural members that incorporate FRP material in conjunction with dissimilar materials have been developed and tested. Deskovic et al., (1995) proposed the design of a hybrid FRP-concrete structural member intended for flexural loading, consisting of a layer of normal strength concrete cast overtop a Glass FRP (GFRP) hollow beam section, with a layer of Carbon FRP (CFRP) sheet bonded onto the exterior bottom flange of the GFRP. It was demonstrated that by utilizing materials where they perform best in the designed cross-section, it could reduce material costs, increase section stiffness and strength as well as incorporate pseudo-ductility into the hybrid member, providing for advanced warning signs prior to structural failure. Nordin and Täljsten (2003) researched a hybrid beam composed of a GFRP pultruded I-beam section, strengthened on the bottom flange with a CFRP sheet with a rectangular normal strength concrete block above the I-beam to resist compressive forces, which showed that epoxy adhesive performed better than steel shear connectors between the concrete and the top flange of the I-beam. Fam and Skutezky (2006) also performed experimental testing on hybrid beams and found that the presence of concrete fill within the interior of the GFRP

First Middle East Conference on Smart Monitoring,
Assessment and Rehabilitation of Civil Structures
8 – 10 February 2011, Dubai, UAE

SMAR 2011

tube significantly increased the stiffness of the member with minimal influence on the overall strength; shear studs embedded in the interior concrete performed better than those without concrete embedment due to insufficient fixity leading to deflection when bending and shear forces are applied. Research showed that the critical shear span-to-depth ratio where tension failure of the GFRP bottom flange and web buckling of the GFRP occurs at the same time is equal to 4. Honickman and Fam (2009) developed and tested hybrid girders using trapezoidal pultruded GFRP sheet pile sections, with results indicating that epoxy adhesive bonding to wet concrete had a similar level of bond strength compared to the bonded aggregate system and GFRP shear studs. In this experiment, the critical shear span-to-depth ratio was 4.2. Mutsuyoshi et al., (2009) used hybrid FRP I-beam with GFRP sheets used in the web and a combination of CFRP and GFRP sheets at varying ratios in the top and bottom flanges. Shear connections for both cast-in-place and precast concrete were tested, achieving composite action that significantly increased the stiffness of the strength of the hybrid FRP beam. Due to the importance of an effective bonding system between adjacent materials in a hybrid structural member, numerous researches have been focused on the performance of bonding at material interfaces. Yuan et al., (2004) introduced a closed-form analytical solution capable of predicting the behaviour along the bond interface during debonding. Experimental and analytical results showed that adhesive bonding is capable of providing full composite action between FRP and steel, for adhesive thicknesses up to 5mm (Keller and Gürtler, 2006). Cho et al., (2010) researched the bonding between stay-in-place concrete and FRP plates using an epoxy bonded coarse sand coated interface tested under double shear and tension pull-out tests, it was found that the optimal aggregate density was 4 kg/m^2 with an aggregate size between 4 – 9.52mm.

2   MATERIALS

Pultruded GFRP hollow box section beams were used, fabricated with internal glass strand rovings for longitudinal strength as well as continuous strand glass mats or stitched reinforcements for transverse strength. It had manufacturer specified ultimate tensile strength of 207 MPa, elastic modulus of 17.2 GPa, with an ultimate strain of 0.012 (Strongwell 2009a). Experimental results from tension coupon tests showed ultimate tensile strength of 321 MPa, elastic modulus of 26.4GPa and ultimate strain equal to 0.012. GFRP shear studs used had specified single shear strength of 7.11 kN (Strongwell 2009b).

From the manufacturer specifications, the UHPC has a modulus of elasticity that can range from between 50 to 70 GPa with compressive strength at 24 hours equal to 30MPa and ultimate compressive strength between 150 to 180 MPa at 28 days. With additional heat curing, the strength can exceed 200 MPa (Lafarge 2007). Experimental compression test results with a total of 22 specimens showed an average compressive strength of 140MPa with a standard deviation of 22 MPa; the modulus of elasticity was 55.7 GPa with a standard deviation of 9.8 GPa. The tests were performed in accordance with ASTM C39 where calculations used equations provided by ASTM C469.

The SFRP sheet is composed of unidirectional brass-coated ultra-high strength twisted steel wires assembled into cords, where each cord has three 0.35 mm diameter straight wires wrapped at a high twist angle with two additional wires. These cords are placed side-by-side into a sheet form that can then be impregnated by resin. Each sheet is made up of 20 aligned steel cords per 25.4 mm (7.87 cords/cm). Individual cords are 0.89 mm in diameter with a breaking load of 1539N, modulus of elasticity equal to 160 GPa and ultimate failure strain of 0.021. When impregnated with resin, the composite SFRP sheet has a thickness of 1.23mm and a net cross-section of 0.38mm^2/mm. Published manufacturer material properties for the composite sheet indicate tensile strength equal to 985 MPa with a modulus of elasticity of 66.1 GPa (Hardwire

First Middle East Conference on Smart Monitoring,
Assessment and Rehabilitation of Civil Structures
8 – 10 February 2011, Dubai, UAE

SMAR 2011

2010). Experimental tension coupon test results for the tensile strength and modulus of elasticity provided values of 936 MPa with a standard deviation of 150MPa and 65.3 GPa with a standard deviation of 7 GPa, respectively. These tests and calculations were performed in accordance with ASTM D3039. The CFRP sheet used is a unidirectional carbon fabric, with a modulus of elasticity of 230 GPa and ultimate tensile strength of 3790 MPa. According to the manufacturer, the composite sheet has a thickness of 1.0 mm, modulus of elasticity of 95.8 GPa and ultimate tensile strength of 986 MPa (Fyfe 2009a). Three types of epoxy adhesives were used. Epoxy Type A (Sikadur® 330) is a moisture intolerant epoxy used for impregnating the SFRP sheets. It has a tensile strength of 30 MPa, modulus of elasticity of 3.8 GPa and ultimate tensile strain of 0.015 (Sika 2007). Epoxy Type B (Sikadur® 32 HI-MOD) is a moisture insensitive epoxy used at the interface between the UHPC and the GFRP beam, applied directly in Phase I specimens and used for bonding silica sand in Phase II specimens. It has a tensile strength of 48 MPa, modulus of elasticity of 3.7 GPa and ultimate tensile strain of 0.019 (Sika 2008). Epoxy Type C (Tyfo® S) was used to bond the CFRP sheets; it has a tensile strength of 72.4 MPa, modulus of elasticity of 3.18 GPa and ultimate tensile strain of 0.051 (Fyfe 2009b).

3   DESCRIPTION OF SPECIMENS

3.1   Design

The design is based on stiffness, strength and ductility requirements by taking advantage of the hybrid FRP-UHPC concept. The primary objective in the design of the hybrid beam system is the integration of pseudo-ductility into a system of high performance materials, which all perform in a nearly linear-elastic manner. The use of the high performance materials in a composite beam will take advantage of their high strength-to-weight ratio, thereby reducing the overall cross-sectional area and total weight of the structural member. A thin layer of UHPC is cast overtop the top flange of the GFRP hollow box section with one single sheet of either SFRP or CFRP bonded to the bottom flange for flexural strengthening. The concrete is designed to carry the compressive stresses in the section, and will eliminate the use of a large GFRP top flange area, thereby reducing the cost of the GFRP material and increasing the stiffness of the section. Through the different investigated bonding systems, the concrete will provide full lateral support to the top flange of the GFRP box and the composite action between the concrete and the top flange will avoid potential lateral buckling of this flange under high compressive stresses. The details of the bonding system used is provided in Section 3.3. Also the high deflection of the GFRP box section (if used alone) is greatly reduced by the addition of the high stiffness FRP materials on the tension side. The concrete cast at the top flange will carry the compressive stresses and the epoxy bonded FRP sheets to the bottom flange will carry the tensile stresses, where the GFRP hollow box section will carry the shear stresses and is used as stay-in-place formwork for the wet concrete. When placed under flexural load, it is expected that, at ultimate, progressive failure will occur, with either rupture of the FRP tensile sheet or crushing of the UHPC layer prior to failure of the GFRP material. To prevent bearing failure at the supports, UHPC end blocks were cast within the ends of the box at to a depth of 180 mm.

3.2   Beam Dimensions and Cross-section

The GFRP hollow box section beam used has an outer height and width of 228.6 mm and 152.4 mm, respectively, with an all-around thickness of 11.11 mm. The height of the UHPC layer above the GFRP beam is 53 mm. The width of the UHPC layer is 187.4 mm and 222.4 mm for the beams reinforced with CFRP and SFRP sheets, respectively. The difference in the UHPC is due to the design of the beams where the gross laminate area of the CFRP and SFRP is not

First Middle East Conference on Smart Monitoring,
Assessment and Rehabilitation of Civil Structures
8 – 10 February 2011, Dubai, UAE

SMAR 2011

identical so that different UHPC area is required to provide a balance of forces in the cross-section that would result in the positioning of the neutral axis within the top flange of the GFRP box for all beam. Cross-section of the beams in both Phase I and II are shown in Figure 1.
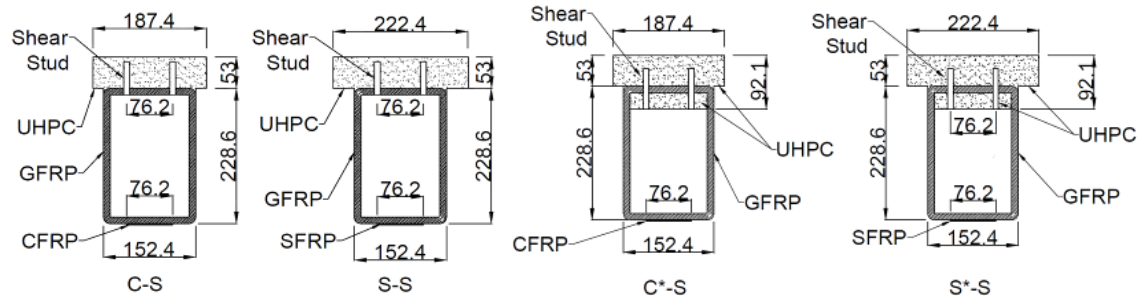
Figure 1. Cross-section of Phase I beams (C-S) and Phase II beams (C*-S and C*S).

3.3 *Bonding at Interface*

Different bonding mechanisms are used at the interface between the UHPC and the GFRP. In Phase I, a thin layer of Epoxy Type B is applied onto the top surface of the GFRP beam just prior to casting the UHPC layer on top. For Phase II beams, coarse silica sand is bonded to the top of the GFRP beam using Epoxy Type B, allowed to cure for 7 days, before casting the UHPC layer above. Both systems were used in conjunction with 9.5 mm diameter GFRP studs, spaced at 100 mm and 75 mm in the longitudinal and transverse direction, respectively, though in the case of Phase II beams, an UHPC layer of approximately 28 mm deep was cast below the top flange of the GFRP within the interior of the box section in order to provide additional anchorage to the GFRP shear studs. This additional layer of UHPC does not contribute to the strength of the beam at ultimate due to the fact that the location of the neutral axis is above the UHPC, causing it to be subjected to tension forces. At failure, tension cracks formed, resulting in the UHPC layer within the GFRP box beam to possesses negligible tension resistance and it can be correctly assumed that ultimate strength of Phase II beams would be quite similar to that of Phase I beams. Six additional GFRP anchor rods were also used in each UHPC end block to provide additional anchorage between the UHPC layer on top of the GFRP beam and the end block. The bond systems are shown in Figure 2.
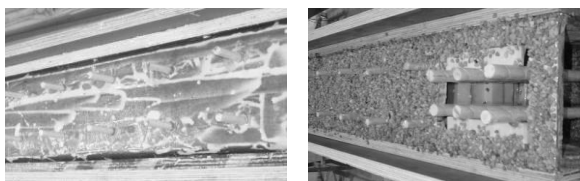
Figure 2. Interface bonding system for Phase I (left) and Phase II (right) beams.

4 TEST SET-UP AND INSTRUMENTATION

The hybrid beams were simply supported and tested under four-point static loading up until failure, using displacement control mode. Each beam was 2900 mm long, from the centers of the two supports. Twelve strain gauges were used on every beam, with two positioned at midspan at the top and bottom of the cross-section, one at the bottom below each point load and one halfway between the support and the point load, also at the bottom of the beam. Three additional strain gauges were positioned at midspan at quarter depth along the height of the GFRP hollow box section, with the final gauge located mid-depth of the UHPC layer at midspan. Linear Variable Displacement Transducers (LVDTs) were positioned at midspan and at the point loads to measure vertical displacement.

First Middle East Conference on Smart Monitoring,
Assessment and Rehabilitation of Civil Structures
8 – 10 February 2011, Dubai, UAE

SMAR 2011

5   EXPERIMENTAL RESULTS

5.1   Phase I Beams: C-S and S-S

Both Phase I beams, the hybrid CFRP-UHPC-GFRP beam (C-S) and the hybrid SFRP-UHPC-GFRP beam (S-S) failed as result of debonding at the interface between the UHPC and the top flange of the GFRP. The beams behaved in a linear elastic manner up until debonding; after debonding, higher applied load resulted in increasingly greater deflections. Debonding of the C-S and S-S beams produced a loss in complete composite behavior between the UHPC and the GFRP beam, where two neutral axis were present within the middle of the two materials. Consequently, tension cracks were present at the bottom of the UHPC layer below the location of the point load. At ultimate failure, both beams experienced web buckling near midspan between the two point loads. Additional information on the failure of the Phase I beams can be found in Chen and El-Hacha (2010). Beam C-S reached a peak load of 222 kN prior to bonding, with a CFRP tensile strain of 5568 με, UHPC strain of 1922 με and midspan deflection of 29 mm, after which a drop in the load carried drop suddenly. Upon continued loading, ultimate failure of the beam occurred at a load of 183 kN, with a maximum CFRP tensile strain of 6486 με, UHPC compressive strain of 1006 με and midspan deflection of 50 mm. The loss of complete composite action resulted in reduced compressive strain at failure compared to that experienced at peak load. Due to the fact that no strain gauges was positioned at the debonding interface, strain values at the UHPC-GFRP interface was obtained using linear extrapolation of the available data; this method was used for both the C-S and S-S beams. The strain profile and distribution of Beam C-S is shown in Figure 3, with photographs of the beam provided in Fig. 4.
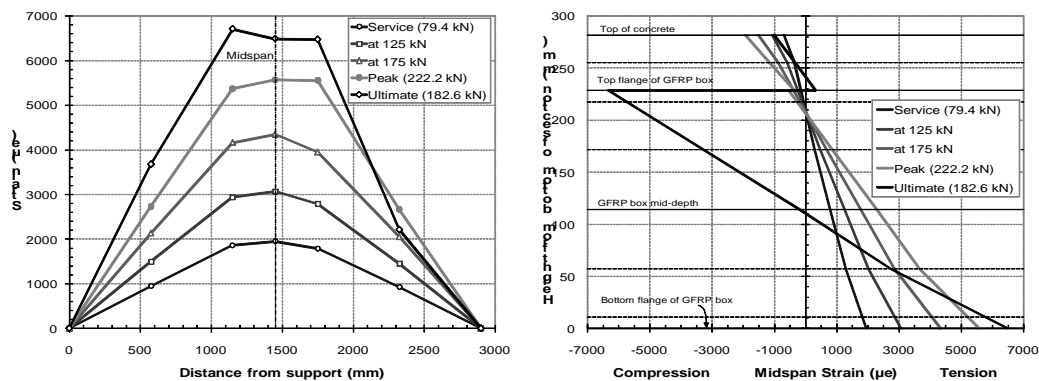
Figure 3. Strain profile (left) and strain distribution (right) for Beam C-S.

| (a) | (b) | (c) | (d) |
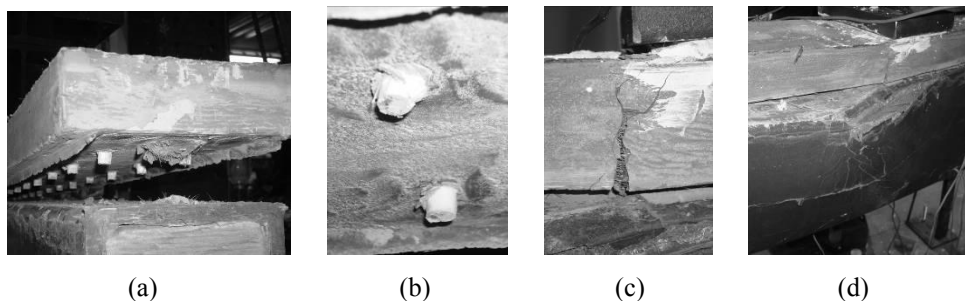
Figure 4. Photographs of Beam C-S: debonding (a and b), tension crack (c) and web buckling (d)

The S-S beam experienced initial debonding at a load of 124 kN, where the SFRP tensile strain was 2955 με, the UHPC compressive strain was 726 με with a midspan deflection of 15 mm. This was followed by further debonding at 133 kN, with SFRP tensile strain of 3546 με, UHPC compressive strain of 891 με and midspan deflection of 20mm, before ultimate failure occurred

First Middle East Conference on Smart Monitoring,
Assessment and Rehabilitation of Civil Structures
8 – 10 February 2011, Dubai, UAE

SMAR 2011

at an applied load of 183 kN. At failure, the SFRP tensile strain was 6876 µε, the maximum UHPC strain was 782 µε and the midspan deflection was 54 mm. The strain profile and distribution are shown in Figure 5 followed by photographs of the beam in Figure 6.
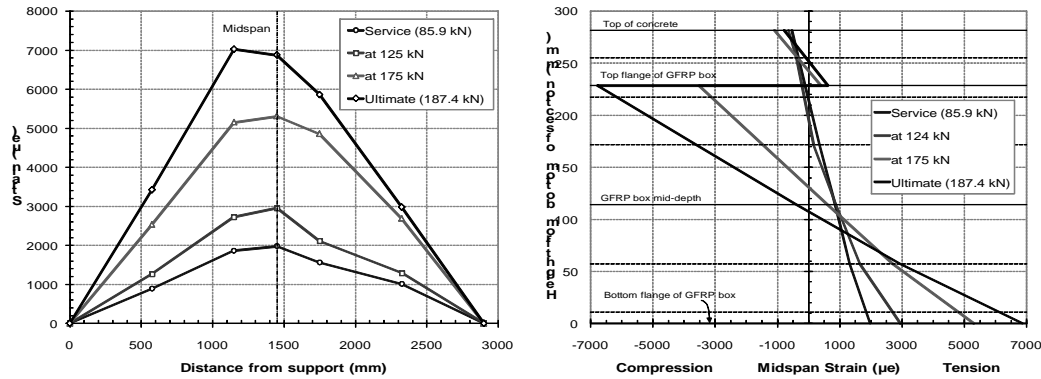
Figure 5. Strain profile (left) and strain distribution (right) for Beam S-S.
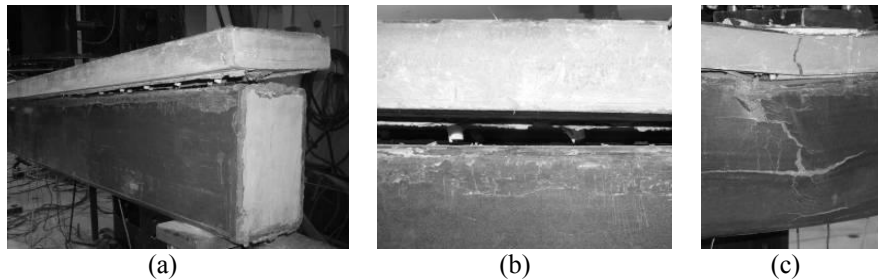
Figure 6. Photographs of Beam S-S: debonding (a – b) and web buckling with UHPC tension crack (c).

5.2   *Phase II Beams: C*-S and S*-S*

Phase II beams did not experience any debonding along the interface between the UHPC and the top flange of the GFRP but rather failed due to shearing of the GFRP webs. The beams behaved linear elastically until ultimate failure. Flexural cracks were present at the base of the beam between the two point loads as well as shear cracks at approximately mid-depth of the GFRP beam in the shear span when the load applied exceeded 335 kN. At failure, the flange-web connection in the GFRP beam ruptures at the end support of the beam, causing complete separation. Beam C*-S reached an ultimate load of 341 kN, with the CFRP tensile equal to 10761 µε, UHPC compressive strain of 2980 µε and midspan deflection of 49 mm. The strain profile and distribution of Beam C*-S is given in Figure 7, with photographs provided in Fig 8.
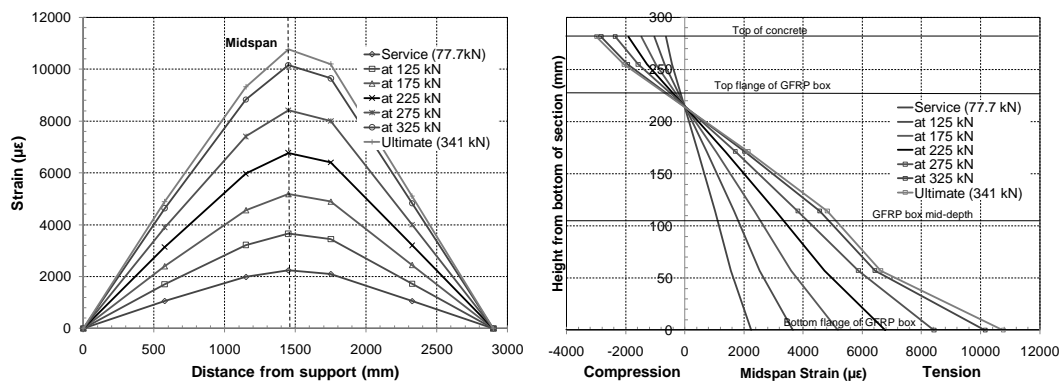
Figure 7. Strain profile (left) and strain distribution (right) for C*-S beam.

First Middle East Conference on Smart Monitoring,
Assessment and Rehabilitation of Civil Structures
8 – 10 February 2011, Dubai, UAE

SMAR 2011
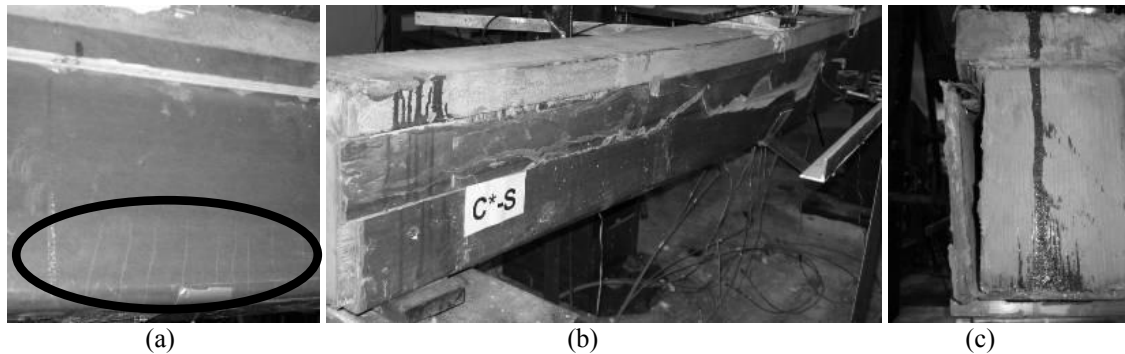
Figure 8. Photographs of Beam C*S: flexural crack (a), beam failure (b) and flange-web connection (c)

Beam S*-S attained an ultimate load of 383 kN, where the SFRP tensile strain was 10050 µε, the UHPC compressive strain was 2672 µε with a midspan deflection of 51 mm. The strain profile and distribution of Beam S*-S is shown in Figure 9; Figure 10 shows photographs of Beam S*-S at failure.
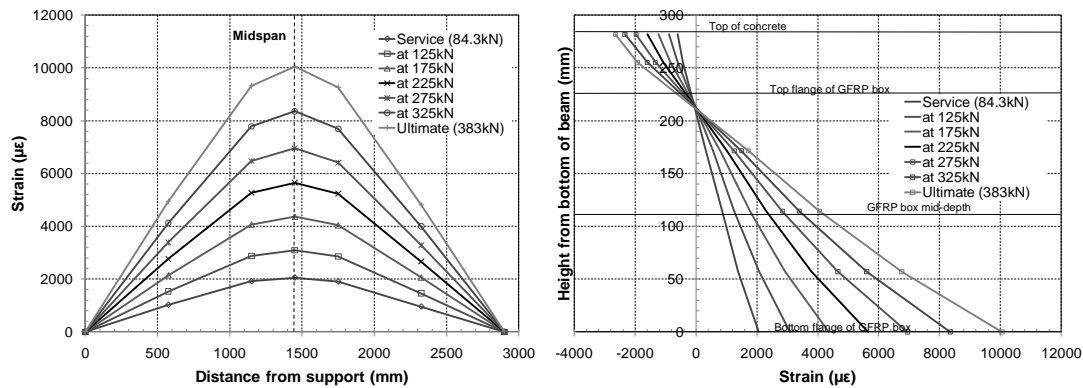
Figure 9. Strain profile (left) and strain distribution (right) for S*-S beam.
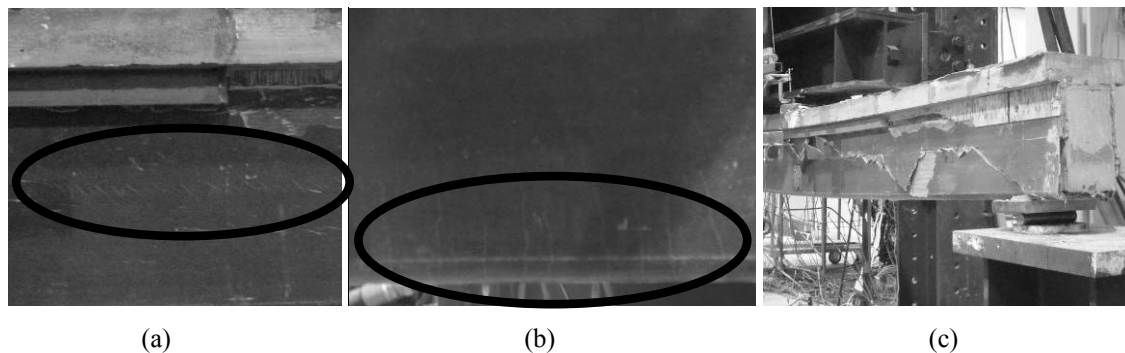
Figure 10. Photographs of Beam S*-S: shear crack (a), flexural crack (b) and beam failure (c).

6   DISCUSSION

The addition of UHPC and FRP tension sheets to the GFRP box beam greatly increased the performance of both Phase I and II beams. For the Phase II beams, where premature debonding did not occur, the UHPC contributed an additional 25% to the stiffness of the beam with the tension sheets contributing approximately 9% more. The increase in flexural strength was approximately three-fold. Comparison of the load-strain and load-deflection curves for all beams, including the GFRP box beam tested alone, is given in Figure 11.

First Middle East Conference on Smart Monitoring,
Assessment and Rehabilitation of Civil Structures
8 – 10 February 2011, Dubai, UAE

SMAR 2011
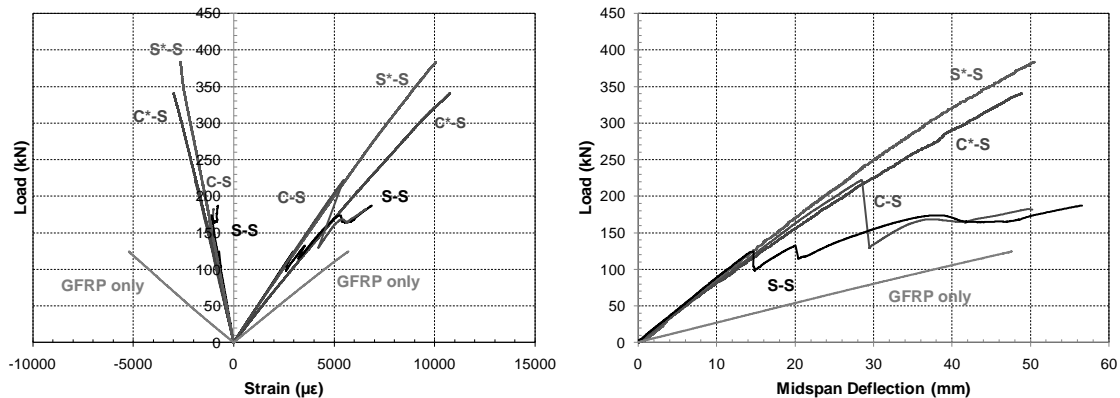
Figure 11. Load-strain and load-deflection of all beams.

The design of the beams from Phase I and II are structurally identical, in terms of flexural strength and member stiffness, except for the bond method used between the UHPC and the GFRP beam. From the experimental results, it can be seen that Phase II beams attained ultimate loads that substantially surpassed that of Phase I beams. Beams C-S and S-S in Phase I of testing did not reach their maximum load carrying capacity due to premature debonding failure. Both of the Phase II beams failed at nearly identical ultimate tensile and compressive strains; however, Beam S*-S achieved a higher load carrying capacity and stiffness. After testing, both beams were closely inspected and it was found that the exterior of the C*-S had slight discolorations on the web sides which was due to outdoor storage of the GFRP box at the manufacturer plant that could have caused a reduction in the flexural strength of the GFRP box beam at ultimate. Further material testing of the GFRP box beam will be performed to verify this assumption.

The price of the two types of tensile sheets used, CFRP and SFRP, including the cost of epoxy, was $19 and $12, respectively. Compared with the unstrengthened GFRP box beam alone, where the ultimate load attained was 124kN, the cost effectiveness, determined by the ratio between the percent increase in strength and the total construction cost, of Beam C*-S and Beam S*-S is 1.23 and 1.32, respectively, noting that in this particular case, the construction cost does not include the GFRP box beam and the workmanship, which is a common element in all beams. From this cost effectiveness comparison, it is shown that the hybrid beam strengthened with SFRP sheet is the more economical option in terms of strength improvement and material cost. The hybrid beam strengthened with SFRP sheet attained the higher ultimate load carrying capacity with the lower cost of the system.

7   CONCLUSIONS

Good bonding at the interface between UHPC and GFRP in a hybrid beam subjected to flexural loading can be achieved using a layer of adhesive bonded coarse silica sand in conjunction with GFRP shear studs, which were used in Phase II beams. Comparison of the beams in Phase II of testing showed that the hybrid UHPC-GFRP beam strengthened with SFRP sheet outperformed the hybrid UHPC-GFRP beam strengthened with CFRP sheet in terms of ultimate strength reached and member stiffness; in addition, cost effectiveness analysis showed the SFRP reinforced hybrid beam is more efficient than the CFRP reinforced hybrid beam. Debonding did not take place in Phase II specimens as compared to Phase I beams, though the expected pseudo-ductile failure, where rupture of the tensile reinforcing sheet or crushing of the concrete prior to ultimate structural failure, did not occur.

First Middle East Conference on Smart Monitoring,
Assessment and Rehabilitation of Civil Structures
8 – 10 February 2011, Dubai, UAE

SMAR 2011

8   ACKNOWLEDGEMENTS

9   REFERENCES

ASTM Standard C39-01. 2001. Standard Test Method for Compressive Strength of Concrete Cylindrical Specimens. . ASTM International, West Conshohocken, PA, USA.

ASTM Standard C469-94. 1994. Standard Test Method for Static Modulus of Elasticity and Poisson's Ratio of Concrete in Compression. . ASTM International, West Conshohocken, PA, USA.

ASTM Standard D3039-00. 2000. Standard Test Method for Tensile Properties of Polymer Matrix Composite Materials. . ASTM International, West Conshohocken, PA, USA.

Chen, D, and El-Hacha, R. 2010. Flexural Behaviour of Hybrid FRP-UHPC Girders under Static Loading. Proceedings of the 8th International Conference on Short and Medium Span Bridge (SMSB 2010), Niagara Falls, Canada, August 2-7, 2010, (CD-Rom, 10p.)

Cho, JR, Cho, K, Park, SY, Kim, ST, and Kim, BS. 2010. Bond Characteristics of Coarse Sand Coated Interface between Stay-in-Place Fibre-Reinforced Polymer Formwork and Concrete Based on Shear and Tension Tests. Canadian Journal of Civil Engineers, 37: 706-718.

Deskovic, N, Triantafillou, TC, and Meier, U. 1995. Innovative Design of FRP Combined with Concrete: Short-Term Behavior. Journal of Structural Engineering, 121 (7): 1069-1078.

Fam, A, and Skutezky, T. 2006. Composite T-Beams using Reduced-Scale Rectangular FRP Tubes and Concrete Slabs. Journal of Composites for Construction, 10(2): 172-181.

Fyfe. 2009a. Tyfo® SCH-41 Composite Product Data Sheet . Fyfe Co. LLC. San Diego, CA, USA.

Fyfe. 2009b. Tyfo® S Saturant Epoxy Product Sheet . Fyfe Co. LLC. San Diego, CA, USA.

Hardwire. 2010. 3X2 Cord Properties - Metric. Hardwire® LLC.   Pocomoke, MD, USA. www.hardwirellc.com

Honickman, H, and Fam, A. 2009. Investigating a Structural Form System for Concrete Girders Using Commercially Available GFRP Sheet-Pile Sections. Journal of Composites for Construction, 13(5): 455-465.

Hai, ND, Mutsuyoshi, H, Asamoto, S, and Matsui, T. 2010. Structural Behavior of Hybrid FRP Composite I-Beam. Construction and Building Materials, 24(6): 956-969.

Keller, T, and Gürtler, H. 2006. Design of Hybrid Bridge Girders with Adhesively Bonded and Compositely Acting FRP Deck. Composite Structures, 74(2): 202-212.

Lafarge. 2007. Fiche de caractéristiques techniques. Lafarge Canada. Calgary, AB, Canada.

Lafarge. 2008. Ductal® Mechanical Performance. Lafarge Canada. Calgary, AB, Canada.

Nordin, H and Täljsten, B. 2004. Testing of Hybrid FRP Composite Beams in Bending. Composites: Part B, 35(1): 27-33.

Sika. 2007. Sikadur® 330 Product Data Sheet. Sika Canada Inc. Pointe-Claire, QC, Canada.

Sika. 2008. Sikadur® 32 Hi-Mod Product Data Sheet. Sika Canada Inc. Pointe-Claire, QC, Canada

Strongwell. 2009a. EXTREN® Fiberglass Structural Shapes and Plate. Strongwell Corporation. Bristol, VA, USA.

Strongwell. 2009b. FIBREBOLT® Fiberglass Studs and Nuts. Strongwell Corporation, Bristol, VA, USA.

Yuan, H, Teng, JG, Seracino, R, Wu, ZS, and Yao, J. 2004. Full-Range Behavior of FRP-to-Concrete Bonded Joints. Engineering Structures, 26(5): 553-565.